Age-Dependent Modulation of Layer V Pyramidal Neuron Excitability in the Mouse Primary Motor Cortex by D1 Receptor Agonists and Antagonists

Valentin Plateau, Jérôme Baufreton, Morgane Le Bon-Jégo

NEUROSCIENCE
RESEARCH ARTICLE
V. Plateau et al. / Neuroscience 536 (2024) 21–35

Age-Dependent Modulation of Layer V Pyramidal Neuron Excitability in the Mouse Primary Motor Cortex by D1 Receptor Agonists and Antagonists

Valentin Plateau, Jérôme Baufreton and Morgane Le Bon-Jégo *

Université de Bordeaux, Institut des Maladies Neurodégénératives, 33076 Bordeaux, France

CNRS UMR 5293, Institut des Maladies Neurodégénératives, 33076 Bordeaux, France

Abstract—The primary motor cortex (M1) receives dopaminergic (DAergic) projections from the midbrain which play a key role in modulating motor and cognitive processes, such as motor skill learning. However, little is known at the level of individual neurons about how dopamine (DA) and its receptors modulate the intrinsic properties of the different neuronal subpopulations in M1 and if this modulation depends on age. Using immunohistochemistry, we first mapped the cells expressing the DA D1 receptor across the different layers in M1, and quantified the number of pyramidal neurons (PNs) expressing the D1 receptor in the different layers, in young and adult mice. This work reveals that the spatial distribution and the molecular profile of D1 receptor-expressing neurons (D1+) across M1 layers do not change with age. Then, combining whole-cell patch-clamp recordings and pharmacology, we explored *ex vivo* in young and adult mice the impact of activation or blockade of D1 receptors on D1+ PN intrinsic properties. While the bath application of the D1 receptor agonist induced an increase in the excitability of layer V PNs both in young and adult, we identified a distinct modulation of intrinsic electrical properties of layer V D1+ PNs by D1 receptor antagonist depending on the age of the animal.

Key words: D1 receptor, dopamine, excitability, primary motor cortex, pyramidal neurons.

INTRODUCTION

Dopamine (DA) is a neuromodulator playing a key role in numerous physiological functions, such as cognitive (Chudasama and Robbins, 2004; for reviews see Nieoullon, 2002; Floresco, 2013), reward (Yokel and Wise, 1975; Michely et al., 2020; for review see Botvinick and Braver, 2015) and motor processes (Ungerstedt et al., 1969; for reviews see Salamone, 1992; Alm, 2021). The dopaminergic (DAergic) system is of high importance and the consequences of its dysregulation are best illustrated by some diseases, notably Parkinson's disease (Bernheimer and Hornykiewicz, 1965; for reviews see Bernheimer et al., 1973; Albin et al., 1989; Nambu et al., 2015), schizophrenia (for reviews see Davis et al., 1991; Brisch et al., 2014; Grace, 2016) and depression (for reviews see Brown and Gershon, 1993; Grace, 2016). Thus, the role of DA in the striatum and the prefrontal cortex (PFC) has been well documented (D'Ardenne et al., 2012; for reviews see Diamond, 1996; Ott and Nieder, 2019; Robbins and Everitt, 1992; Valjent et al., 2019). However, even if to a lesser extent, the primary motor cortex (M1) also receives DAergic innervation (Descarries et al., 1987; Gaspar et al., 1991), which comes from midbrain DAergic neurons (Hosp et al., 2011). M1 is involved in motor learning and it has been described that learning sophisticated motor sequences such as skill-reaching behavior relies upon DA-dependent structural and synaptic plasticity in M1 (Hosp et al., 2009, 2011; Guo et al., 2015). Although the architecture of the DAergic system within M1 has been well characterized anatomically in rodents (Descarries et al., 1987; Vitrac et al., 2014; Hosp et al., 2015), the level of understanding of DA action in M1 is rather macroscopic (for review see Cousineau et al., 2022), monitoring global changes at the level of M1. Besides, its functional significance remains debated, in part because the precise location of DA receptors and the modulation exerted by these receptors at the level of individual neurons is poorly understood and sometimes inconsistent.

DA activates two main classes of receptors, the D1-like and the D2-like family which are both present in M1 (Dawson et al., 1986; Lidow et al., 1989; Weiner et al.,

*Corresponding author. Address: Université de Bordeaux, Institut des Maladies Neurodégénératives, 33076 Bordeaux, France.
E-mail address: morgane.jego@u-bordeaux.fr (M. Le Bon-Jégo).

Abbreviations: DA, dopamine; DAergic, dopaminergic; D1+, D1 receptor-expressing neurons; GFP, green fluorescent protein; M1, primary motor cortex; PNs, pyramidal neurons; PFC, prefrontal cortex.

https://doi.org/10.1016/j.neuroscience.2023.11.006
0306-4522/

1991; Gaspar et al., 1995). In M1, it has been shown that pyramidal neurons (PNs) and interneurons express D1 and/or D2 DA receptors (Gaspar et al., 1995; Vitrac et al., 2014; Cousineau et al., 2020; Swanson et al., 2021). Based on their axonal projection, PNs can be divided into 3 major classes in M1, the pyramidal tract neurons (PT) which express the transcription factor Ctip2 (also known as Bcl11b), the intra-telencephalic neurons (IT) which express Satb2 and the cortico-thalamic (CT) neurons mainly located in layer VI (Arlotta et al., 2005; Alcamo et al., 2008; Britanova et al., 2008; Digilio et al., 2015, for review see Molnár and Cheung, 2006; Shepherd, 2013). At the level of M1, some studies investigated the effect of DA receptors on the intrinsic properties of neurons. However, they were more centered on the D2 receptor (Parr-Brownlie, 2005; Vitrac et al., 2014; Cousineau et al., 2020; Swanson et al., 2021, for review see Cousineau et al., 2022). The specific impact of D1 receptors on the activity of PNs in M1 remains elusive. To date, only one recent study has explored in mice the effect of D1 receptor antagonist in M1, with no direct evidence of D1 receptor expression in the recorded neurons (Swanson et al., 2021). Furthermore, the impact of D1 receptor activation in M1 PNs has not yet been investigated, nor has the molecular profile of the PNs expressing the D1 receptor. In the PFC, *ex vivo* electrophysiological recordings have revealed that the activation of the D1 receptors increases the firing properties of subpopulations of PNs (Seong & Carter, 2012), with the majority displaying properties of IT neurons (Anastasiades et al., 2019). Additionally, no study has investigated if the age of the animals can influence the DA modulation of the activity of PNs. Indeed, age is a critical variable as developmental changes continue to occur far beyond the first postnatal weeks.

This study aimed to fill the gap in our understanding of how D1 receptors are expressed in the different layers of M1, and how they impact the intrinsic properties of PNs expressing the D1R (D1+) in the layer V of M1, in young and adult mice. Using the D1-GFP transgenic mouse line, we first mapped in young (P16-P25 old) and adult mice (6–10 weeks old) neurons expressing the D1 receptors according to M1 layers and pyramidal neuronal markers they express (Ctip2 and Satb2). Then using whole-cell patch-clamp recordings coupled to pharmacology, we investigated *ex vivo* in layer V how activation and blockade of the D1 receptor in M1 modulate D1+ PNs intrinsic properties in young and adult animals. This work reveals an age-dependent modulation of the excitability of M1 layer V D1+ PNs by D1 receptors.

EXPERIMENTAL PROCEDURES

Animals

All experiments were performed in accordance with the guidelines of the French Agriculture and Forestry Ministry for handling animals (APAFIS #26 770) and the official European guidelines (Directive 2010/63/UE). Male and female D1-GFP mice (Tg(Drd1-EGFP) X60Gsat) were used, aged between P16 and P25 for young mice and between 6 and 10 weeks for adult mice. Young mice from P16 to P25 have been chosen, as the number of layer V D1 receptor sites is at its maximum at these stages of development in the PFC (Leslie et al., 1991). D1-GFP mice express the GFP under the D1 receptor promoter, enabling the identification of D1-expressing cells. Mice were housed collectively under artificial conditions of light (12/12 h light/dark cycle, light on at 7:00 a.m.), with food and water access *ad libitum*. Experimenters were not blind to animal age or treatment.

Slice preparation

Mice were deeply anesthetized using ketamine and xylazine (100 and 20 mg/kg, i.p., respectively). After the disappearance of all arousal reflexes, a thoracotomy was done to enable the transcardial perfusion of an ice-cooled and oxygenated with carbogen (95% O_2/5% CO_2) cutting solution containing 250 mM sucrose, 2.5 mM KCl, 1.25 mM $NaH_2PO_4{\cdot}H_2O$, 0.5 mM $CaCl_2{\cdot}H_2O$, 10 mM $MgSO_4{\cdot}7H_2O$, 10 mM D-glucose and 26 mM $NaHCO_3$. The brain was then quickly removed and glued to the stage of a vibratome (VT1200S; Leica Microsystems, Germany) and placed into a cutting chamber filled with the cutting solution and oxygenated with carbogen. The brain was then cut into 300 μm thick sections, which were then incubated for 1 hour into a 37 °C warmed ACSF containing 126 mM NaCl, 2.5 mM KCl, 1.25 mM $NaH_2PO_4{\cdot}H_2O$, 2 mM $CaCl_2{\cdot}H_2O$, 2 mM $MgSO_4{\cdot}7H_2O$, 26 mM $NaHCO_3$, and 10 mM D-glucose, 1 mM sodium pyruvate and 4.9 μM L-glutathione reduced and oxygenated with carbogen (~310 mOsm). Slices were then placed at room temperature for 30 minutes before recordings.

Drugs

Drugs were prepared in double-distilled water as concentrated stock solutions, then aliquoted and stored at −20 °C. Drugs were diluted daily at the experimental concentrations and perfused in the recording chamber. In all experiments, glutamatergic AMPA/kainate and NMDA receptors were blocked with 20 μM 6,7-dinitroquinoxaline-2,3-dione (DNQX, Tocris, UK) and 50 μM D-(-)-2-amino-5-phosphonopentanoic acid (APV, Tocris, UK) respectively, and $GABA_A$ receptors were blocked using 10 μM 6-Imino-3-(4-methoxyphenyl)-1(6*H*)-pyridazine butanoic acid hydrobromide (GABAzine, Tocris, UK). To block D1 receptors, 1 μM D1 receptor antagonist (*R*)-(+)-7-Chloro-8-hydroxy-3-methyl-1-phenyl-2,3,4,5-tetrahydro-1*H*-3-benzazepine hydrochloride (SCH 23390, Sigma, France) was used, and to activate D1 receptors, 2.5 μM D1 receptor agonist (±)-6-Chloro-2,3,4,5-tetrahydro-1-phenyl-1*H*-3-benzazepine hydrobromide (SKF 81297, Tocris, UK) was used. Electrophysiological recordings were made 20 minutes after drug application.

Ex vivo electrophysiological recordings

Single slices were placed in a recording chamber continuously perfused with a recording solution

Table 1. List of primary antibodies used.

Antigen	Host	Dilution	Supplier	# Catalog	# Lot
Ctip2	Rat	1:500	Abcam	ab18465	GR3272266-4
GFP	Chicken	1:1000	Aves lab	GFP-1010	GFP3717982
GFP	Chicken	1:1000	Abcam	ab13970	GR3190550-21
Satb2	Mouse	1:300	Abcam	ab51502	GR273053-6

containing 126 mM NaCl, 3 mM KCl, 1.25 mM NaH2PO4·H2O, 1.6 mM CaCl2·H2O, 2 mM MgSO4·7H_2O, 10 mM D-glucose and 26 mM NaHCO3, oxygenated with carbogen and heated at 32 °C. D1+ PNs were visualized under IR-DIC and fluorescence microscopy using a 63X water-immersion objective (W Plan-Apochromat 63X/1.0 VIS-IR, Zeiss) equipped on an axio examiner Z.1 microscope (Zeiss, Germany). PNs were identified by the shape of their cell bodies and then confirmed by their electrophysiological signature. The use of D1-GFP mice enabled us to record only D1+ PNs. Recordings of PNs were made using patch pipettes of impedance between 4–9 MΩ. These pipettes were made from glass capillaries (GC150F10; Warner Instruments, Hamden, CT, USA) pulled with a horizontal pipette puller (P-97; Sutter Instruments, Novato, CA, USA). All recordings were made in the whole-cell configuration using an internal pipette solution containing 135 mM K-gluconate, 3.8 mM NaCl, 1 mM $MgCl_2$·6H_2O, 10 mM HEPES, 0.1 mM Na4EGTA, 0.4 mM Na2GTP, 2 mM MgATP and 5.4 mM biocytin (pH = 7.2, ∼292 mOsm). Recordings were corrected for a junction potential of 13 mV. Experiments were done with a Multiclamp 700B amplifier and digidata 1550B digitizer controlled by clampex 11.0 (Molecular Devices LLC). Recordings were acquired at 20 kHz and low-pass filtered at 4 kHz. Series resistance was monitored throughout the experiment by voltage steps of −5 mV, and data were discarded when the series resistance changed by > 20%.

Histology

Transcardial perfusions were made on mice following the same procedure as described for slice preparation, except the ACSF used did not contain sodium pyruvate and glutathione. The brains were then post-fixed at 4 °C in a solution of PBS 0.01 M containing 4% paraformaldehyde for 24 hours, washed, and cut into 50 μm thick slices with a vibratome (VT1000S; Leica Microsystems, Mannheim, Germany). Slices were then processed for immunohistochemistry labeling. Slices were placed in a blocking buffer for 2 hours, then 48 hours in a solution of PBS 0.01 M/Triton X-100 0.3% containing the primary antibodies (Table 1). Slices were washed three times in PBS 0.01 M, incubated with the secondary antibodies for 2 hours, washed three times again with PBS 0.01 M, and then mounted onto slides in DAPI fluoromount medium (SouthernBiotech). Images were taken with a confocal microscope (Leica TCS SP8, Leica Microsystems, Mannheim, Germany) equipped with an HC PL APO 20x/0.75 IMM CORR CS2 objective (used to take pictures for counting). Confocal images were further processed using Fiji. Counting and colocalization were made manually using a rectangle-delimited M1 area. Layers were delimited by the DAPI and Ctip2 labeling. The delimitation between layer I and layer II-III was placed where a sharp decrease in nuclear DAPI labeling is found. The layer V was placed where there is an increase in Ctip2 labeling intensity. Three slices containing a large part of M1 from three mice were used for counting (Fig. 1A, B; 2A, B).

Data analysis

Electrophysiological data were analyzed using Clampfit 10.7 (Molecular Devices, USA) and Origin 7 (OriginLab, USA). Input-output (F-I) curves were generated by injecting increasing 1 s depolarizing currents (25 pA increments, from −150 pA to 225 pA) and counting the number of evoked action potentials. Input resistance was calculated using Ohm's law when a current of −50 pA was injected. ΔU corresponds to the voltage variation between the baseline and the new voltage recorded due to the current injection. The rheobase was determined by injecting increasing depolarizing currents of 500 ms, with 1 pA increments. Action potential half width and peak amplitude were obtained after detecting each spike with the threshold search in Clampfit 10.7. The action potential threshold was measured as the beginning of the rising slope of the phase plots of the neurons. These phase plots were made at rheobase using Clampfit 10.7. Electrophysiological traces were processed using Origin 7.

Statistics

Statistical analyses were performed using Prism 9.3.1 (GraphPad Software Inc). For paired analysis (*i.e.*, for

Fig. 1. Distribution of D1+ neurons in M1 of young mice. **(A)** Image of a coronal section at the level of M1 showing the D1+ neurons in a young animal. **(B)** Laminar distribution of D1+ cells in M1 of young mice. For each category, the darker the color, the deeper the layer. **(C)** Left, schematic of a coronal slice containing M1. The red rectangle indicates the area imaged in D. Right, distribution in % of all D1+ cells in M1 according to their molecular identity. **(D)** Example of the labeling obtained for D1 (green), Ctip2 (blue), and Satb2 (magenta) in M1. **E.** Enlarged view of layer V at the level of the red-dotted square in D for each molecular marker. The brown arrowheads indicate neurons positive for D1, Ctip2 and Satb2 labeling. **(F)** Distribution of D1 positive only (green), D1 and Ctip2 positive only (blue), D1 and Satb2 positive only (magenta), and D1, Ctip2 and Satb2 positive (brown) cells in M1 layers. For each category, the darker the color, the deeper the layer. Data are given as mean ± SEM.

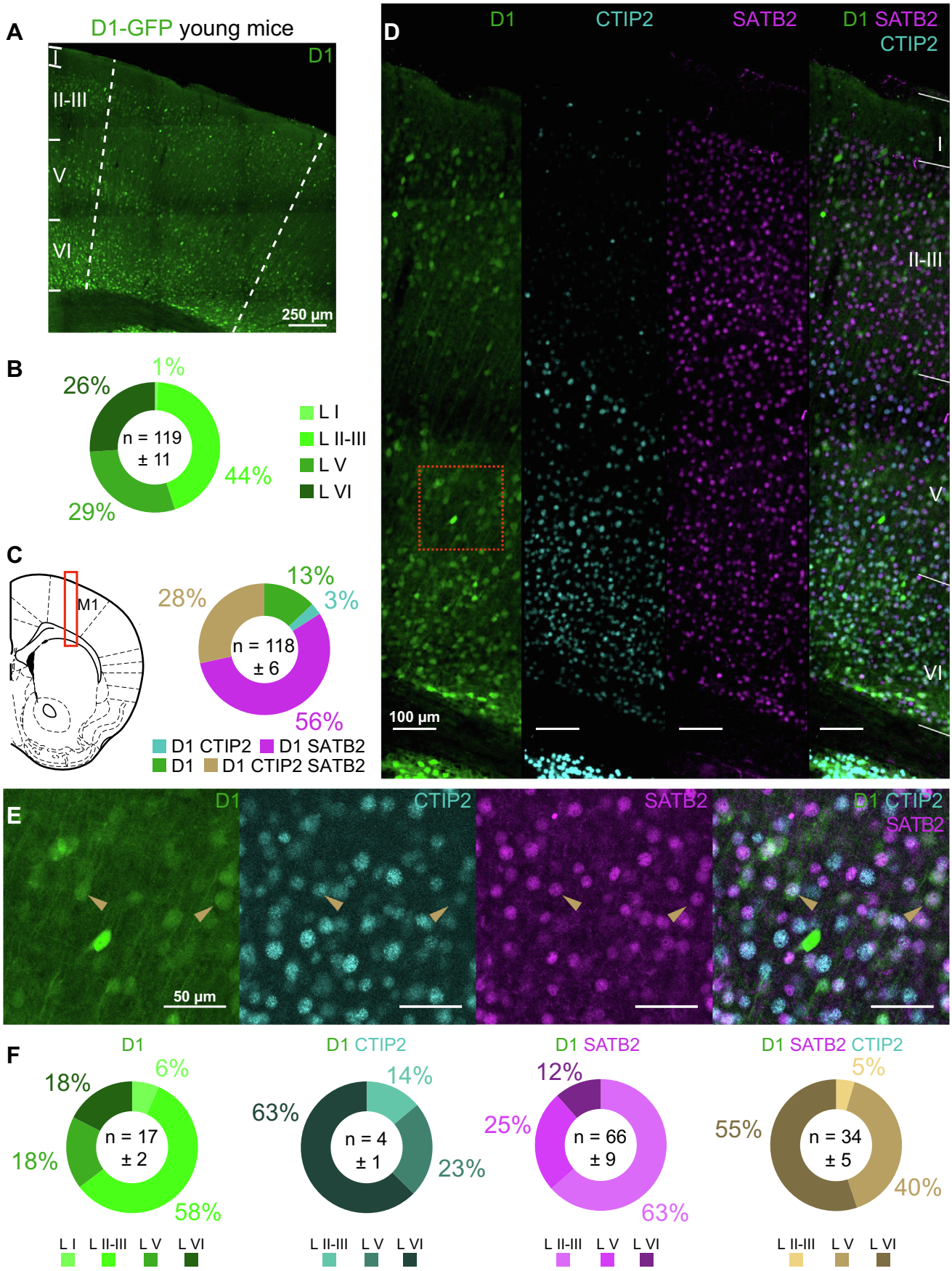
A
D1-GFP young mice
D1
I
II-III
V
VI
250 µm
B
1%
26%
n = 119
± 11
44%
29%
L I
L II-III
L V
L VI
C
M1
13%
28%
3%
n = 118
± 6
56%
D1 CTIP2
D1 SATB2
D1
D1 CTIP2 SATB2
D
D1
CTIP2
SATB2
D1 SATB2
CTIP2
I
II-III
V
VI
100 µm
E
D1
CTIP2
SATB2
D1 CTIP2
SATB2
50 µm
F
D1
18%
6%
n = 17
± 2
18%
58%
L I
L II-III
L V
L VI
D1 CTIP2
14%
63%
n = 4
± 1
23%
L II-III
L V
L VI
D1 SATB2
12%
25%
n = 66
± 9
63%
L II-III
L V
L VI
D1 SATB2 CTIP2
5%
55%
n = 34
± 5
40%
L II-III
L V
L VI

membrane resting potential, rheobase, action potential peak amplitude, action potential threshold, input resistance, and action potential half-width) Wilcoxon signed rank tests (WSR) were performed. In this case, the black dotted line represents the mean ± standard error to the mean (SEM) of all neurons, and the transparent-colored lines represent individual neurons. For firing frequency, two-way multiple comparisons ANOVA followed by a Bonferroni post hoc were made. In all tests, the level of significance was set at $p < 0.05$. The effect size has been calculated using Cohen's d, following the formula: $d = \frac{\text{mean(control)} - \text{mean(treated)}}{pooled\ \ sd}$. The pooled sd was calculated as follow: $\sqrt{\frac{sd(control)^2 + sd(treated)^2}{2}}$. d values are given as absolutes. An effect size < 0.1 is trivial, one between 0.1 and 0.3 is small, one between 0.3 and 0.5 is moderate, and one > 0.5 is considered large, according to Cohen (Cohen, 1988). Data are represented as mean ± SEM in the figures. Details about statistical tests, *p*-values and effect size are shown in Tables 2–4.

RESULTS

The distribution of D1 receptor expressing cells in M1 is similar in young and adult mice

Taking advantage of the D1-GFP transgenic mice in which the GFP is expressed under the control of the D1 receptor promoter, we first performed a quantitative layer-based mapping of M1 neuronal populations expressing the D1 receptor in young and adult mice. The analysis of the GFP fluorescence in M1 brain slices revealed that D1+ cells were distributed in all M1 cortical layers and with a similar distribution in young and adult mice (Fig. 1A, B; 2A, B). In young mice, ~26% of D1 receptor-expressing cells were localized in layer VI, ~29% in layer V, 44% in layers II/III, and less than 1% in layer I (Fig. 1A, B). In adult mice, ~30% of D1+ cells were localized in layer VI, ~34% in layer V, ~35% in layers II/III and less than 1% in layer I (Fig. 2A, B).

To refine the molecular identity of the D1+ cells, we performed immunostaining to quantify the colocalization of GFP with specific markers of two classes of pyramidal neurons. Ctip2 and Satb2 transcription factors were used as molecular markers of PT and IT neurons, respectively (Arlotta et al., 2005; Alcamo et al., 2008; Britanova et al., 2008; Digilio et al., 2015; for review see Molnár and Cheung, 2006). The D1+ neurons were then divided into four categories: the cells expressing only the D1 receptor, neurons expressing the D1 receptor and only Ctip2, those expressing the D1 receptor and only Satb2, and those expressing the D1 receptor and both Ctip2 and Satb2, in young and adult mice (Fig. 1C–F; 2C–F). Most of the D1+ cells in M1 co-expressed Satb2 (around 80% both in young and adult mice) and very few cells co-expressed only Ctip2 (3.3% and 1.83% in young and adult mice, respectively) (Fig. 1C; 2C). The laminar distribution of the cells in the four categories was also similar in young and adult mice (Fig. 1D–F; 2D–F and Table 2). The cells expressing only the D1 receptor were mostly localized in layer II-III, 58.01% in young (Fig. 1D–F) and 52.09% in adult mice (Fig. 2D–F). The few D1+ cells co-expressing only Ctip2 were mainly localized in layer VI both in young (Fig. 1D–F) and adult mice (Fig. 2D–F). The D1+ cells co-expressing Satb2 were mainly localized in layer II–III as they represented 63.46% in young (Fig. 1D–F) and 58.38% in adult mice (Fig. 2D–F) and in layer V (25.03% and 32.63%). Finally, a non-negligible number of D1+ cells co-expressing Ctip2 and Satb2 were also counted. They were mainly found in layer VI of young (55.15%) and adult (56.86%) mice (Fig. 1D–F; 2D–F).

D1 receptor activation increases D1+ PNs excitability both in young and adult animals

We then explored if the DA D1 receptor can modulate the intrinsic electrical properties of individual neurons and whether DAergic modulation of these neurons changes with age. We focused our attention on PNs in layer V, the main output layer of the cortex (Lévesque et al., 1996; Veinante et al., 2000; Hattox and Nelson, 2007; for reviews see Aronoff et al., 2010; Harris and Shepherd, 2015) which is largely innervated by DAergic fibers (Vitrac et al., 2014). Using patch-clamp recording, we first investigated *ex vivo* the effects of the activation of the D1 receptors on D1+ PNs' intrinsic electrical properties in M1 layer V (Figs. 3, 4). Among D1+ cells, PNs were identified on morphological (triangle shape of their cell bodies) and electrophysiological criteria. To prevent a network effect, intrinsic properties of D1+ PNs were recorded while pharmacologically blocking fast glutamatergic and GABAergic transmission using DNQX (50 μM), APV (20 μM), and GABAzine (10 μM). In young animals (Fig. 3), bath application of the D1 agonist SKF 81297 (2.5 μM) changed the intrinsic properties of the D1+ PNs recorded. Many parameters were measured and to assess the treatment effect, not only was calculated the *p*-value, but also the effect size. We observed that D1+ PNs were more excitable as they fired more action potentials in response to current injections from

Fig. 2. Distribution of D1+ neurons in M1 of adult mice. **(A)** Image of a coronal section at the level of M1 showing the D1+ neurons in the brain of an adult mouse. **(B)** Laminar distribution of D1+ cells in M1 of adult mice. For each category, the darker the color, the deeper the layer. **(C)** Left, schematic of a coronal slice containing M1. The pictures in D. are taken from the area delineated by the red-dotted square. Left, distribution in % of all D1+ cells in M1 according to their molecular identity in adult mice. **(D)** Example of the labeling obtained for D1 (green), Ctip2 (blue), and Satb2 (magenta) in M1 of an adult mouse. **(E)** Higher magnification of the layer V of M1 at the level of the red-dotted square in B. for the same molecular markers. The brown arrowheads indicate neurons positive for D1, Ctip2 and Satb2 labeling. **(F)** Distribution of D1 positive only (green), D1 and Ctip2 positive only (blue), D1 and Satb2 positive only (magenta), and D1, Ctip2 and Satb2 positive (brown) cells in M1 layers. For each category, the darker the color, the deeper the layer. Data are given as mean ± SEM.

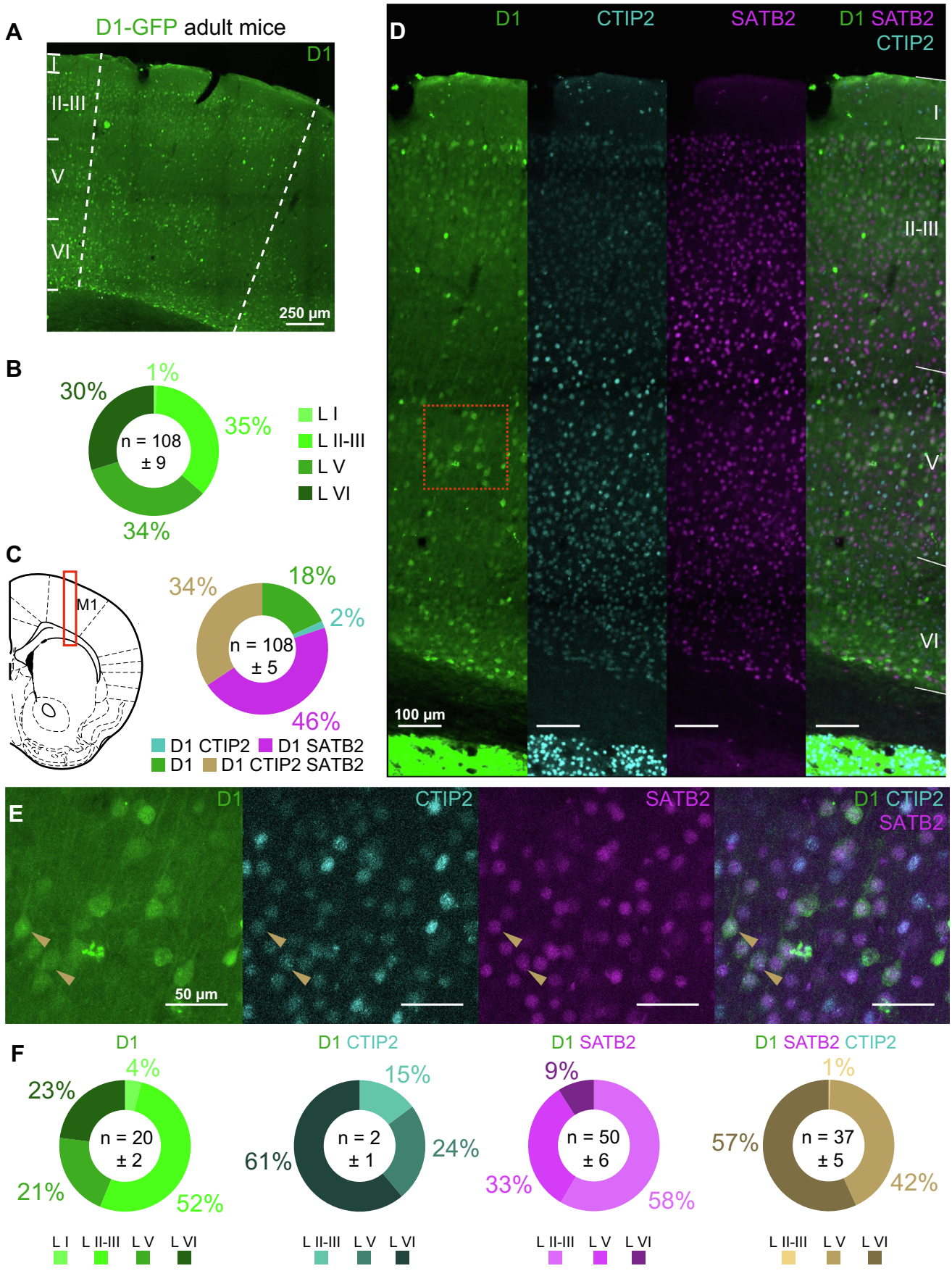
A
D1-GFP adult mice
D1
I
II-III
V
VI
250 µm
B
1%
30%
35%
n = 108
± 9
34%
L I
L II-III
L V
L VI
C
M1
34%
18%
2%
n = 108
± 5
46%
D1 CTIP2
D1 SATB2
D1
D1 CTIP2 SATB2
D
D1
CTIP2
SATB2
D1 SATB2
CTIP2
I
II-III
V
VI
100 µm
E
D1
CTIP2
SATB2
D1 CTIP2
SATB2
50 µm
F
D1
4%
23%
n = 20
± 2
21%
52%
L I
L II-III
L V
L VI
D1 CTIP2
15%
61%
n = 2
± 1
24%
L II-III
L V
L VI
D1 SATB2
9%
n = 50
± 6
33%
58%
L II-III
L V
L VI
D1 SATB2 CTIP2
1%
57%
n = 37
± 5
42%
L II-III
L V
L VI

Table 2. Statistical analysis of the distribution and the molecular identity of the D1 receptor expressing neurons in M1 of young and adult mice.

	D1 only – Young				D1 only – Adult				*p*-value
	n = 9								Mann-Whitney
	Mean	Mean %	SEM	SEM %	Mean	Mean %	SEM	SEM %	
Layer I	1.000	6.639	0.236	1.833	0.778	4.114	0.222	1.067	> 0.999
Layer II/III	9.222	58.015	0.940	3.563	10.111	52.087	1.263	5.088	0.0892
Layer V	3.444	17.851	0.944	3.435	3.889	20.753	0.676	3.602	0.8796
Layer VI	2.889	17.496	0.633	3.007	4.778	23.046	1.470	5.612	0.3081
	D1 Ctip2 only – Young				D1 Ctip2 only – Adult				*p*-value
	n = 9								Mann-Whitney
	Mean	Mean %	SEM	SEM %	Mean	Mean %	SEM	SEM %	
Layer I	0.000	0.000	0.000	0.000	0.000	0.000	0.000	0.000	NA
Layer II/III	0.125	13.889	0.147	7.384	0.222	14.815	0.147	11.264	0.7176
Layer V	0.750	23.512	0.289	7.682	0.444	24.074	0.242	12.763	0.4869
Layer VI	2.625	62.599	1.002	11.729	1.222	61.111	0.434	16.197	0.5923
	D1 Satb2 only – Young				D1 Satb2 only – Adult				*p*-value
	n = 9								Mann-Whitney
	Mean	Mean %	SEM	SEM %	Mean	Mean %	SEM	SEM %	
Layer I	0.000	0.000	0.000	0.000	0.000	0.000	0.000	0.000	NA
Layer II/III	41.625	63.459	4.916	3.049	28.111	58.377	0.949	3.946	0.1297
Layer V	16.375	25.032	1.956	2.453	16.556	32.630	2.062	2.683	0.4503
Layer VI	7.625	11.509	1.047	2.199	5.000	8.992	1.863	3.162	0.1095
	D1 Satb2 Ctip2 – Young				D1 Satb2 Ctip2 – Adult				*p*-value
	n = 9								Mann-Whitney
	Mean	Mean %	SEM	SEM %	Mean	Mean %	SEM	SEM %	
Layer I	0.000	0.000	0.000	0.000	0.000	0.000	0.000	0.000	NA
Layer II/III	1.333	4.535	0.408	1.428	0.111	0.383	0.111	0.383	**0.0078**
Layer V	13.889	40.313	2.312	3.397	15.778	42.758	1.211	3.076	0.5919
Layer VI	18.444	55.152	2.304	3.664	21.222	56.859	1.730	3.078	0.2547

25 pA to 175 pA (Fig. 3B, two-way repeated measures ANOVA, $F_{(9, 72)} = 138.5$, $p < 0.0001$, $n = 9$ and Table 3) in presence of the D1 receptor agonist SKF 81297 (Fig. 3C). Furthermore, the rheobase, action potential threshold, half-width and peak amplitude were significantly lower with the application of D1 receptor agonist SKF 81297 compared to control conditions (Fig. 3D, Wilcoxon signed rank (WSR), $p < 0.05$, $n = 9$ and Table 4). No significant effect was observed concerning the resting membrane potential and the input resistance (Fig. 3D, WSR, $p > 0.05$, $n = 9$).

The effect of D1 receptor activation on layer V M1 D1 + PNs was then assessed in adult mice (Fig. 4). As for young mice, D1 agonist increased the excitability of D1 + PNs as illustrated by the recording of a D1+ PN in response to a 100 pA current injection (Fig. 4C). For current injections from 50 pA to 175 pA, D1+ PNs fired more action potentials in presence of SKF 81297 compared to control conditions (Fig. 4B, two-way repeated measures ANOVA, $F_{(9, 144)} = 306.2$, $p < 0.0001$, $n = 17$). It should be noted, however, that the effect size of D1 receptor activation is slightly smaller in adult than in young mice (Table 3). Moreover, the action potential half width, and the action potential threshold were significantly lower in the presence of SKF 81297 compared to the control condition (Fig. 4D, WSR, $p < 0.05$, $n = 17$). A trend of decreasing input resistance was observed and supported by the moderate effect calculated using the Cohen method (Table 4). No significant effect was observed concerning the resting membrane potential, the rheobase, and the action potential peak amplitude (Fig. 4D, WSR, $p > 0.05$, $n = 17$ and Table 4). These effects were specific to the activation of the receptor as coactivating and blocking the D1 receptor simultaneously did not affect significantly the intrinsic properties of the D1+ PNs (Supplementary Fig. 1).

Blockade of D1 receptor differently impact layer V D1 + PNs intrinsic properties according to the age

We then investigated the effect of blocking the D1 receptor on D1+ PNs' intrinsic properties in M1 layer V (Figs. 5 and 6). In young animals (Fig. 5), bath application of the D1 antagonist SCH 23390 (1 μM) had the opposite effect of the bath application of the D1 agonist on the intrinsic properties of the D1+ PNs recorded. Indeed, we observed a significant decrease in the neuronal excitability of D1+ PNs in the presence of SCH 23390. D1+ PNs fired fewer action potentials in

Table 3. Statistical analysis of the effect of the D1 receptor agonist and antagonist on the firing properties of layer V pyramidal neurons.

		Control young		D1R agonist young		*p*-value	Effect size d
		n = 9				ANOVA2 way	Cohen
		Mean	SD	Mean	SD		
Firing frequency (Hz)	0 pA	0.000	0.000	0.000	0.000	> 0.9999	0.000
	25 pA	0.667	1.658	3.111	3.296	< **0.0001**	0.9370
	50 pA	3.889	3.621	6.778	5.380	< **0.0001**	0.6299
	75 pA	8.000	4.472	11.11	5.231	< **0.0001**	0.6393
	100 pA	11.33	5.523	14.67	5.408	< **0.0001**	0.6099
	125 pA	14.67	5.895	17.33	5.568	< **0.0001**	0.4651
	150 pA	17.56	5.940	19.67	5.895	< **0.0001**	0.3568
	175 pA	20.44	5.747	22.11	5.904	**0.0004**	0.2861
	200 pA	23.00	5.408	23.89	6.412	0.0903	0.1499
	225 pA	24.67	5.568	25.22	6.704	0.4173	0.0902
		Control adult		D1R agonist adult		*p*-value	d
		n = 17				ANOVA2 way	Cohen
		Mean	SD	Mean	SD		
Firing frequency (Hz)	0 pA	0.250	1.000	0.250	1.000	> 0.9999	0.000
	25 pA	0.375	1.500	0.813	2.401	0.7501	0.2118
	50 pA	2.813	3.582	4.250	3.907	**0.0014**	0.4302
	75 pA	6.688	3.928	8.125	4.965	**0.0033**	0.3357
	100 pA	10.63	3.500	11.88	5.149	**0.0076**	0.3162
	125 pA	13.81	3.449	14.94	4.781	**0.0233**	0.2912
	150 pA	16.50	3.688	18.13	5.620	**0.0009**	0.3576
	175 pA	19.19	3.637	20.63	5.548	**0.0051**	0.3106
	200 pA	21.44	3.932	21.88	5.512	0.6216	0.1014
	225 pA	23.63	4.145	23.94	5.767	0.8940	0.0725
		Control young		D1R antagonist young		*p*-value	d
		n = 9				ANOVA2 way	Cohen
		Mean	SD	Mean	SD		
Firing frequency (Hz)	0 pA	0.000	0.000	0.000	0.000	> 0.9999	0.000
	25 pA	0.556	1.667	0.556	1.667	> 0.9999	0.000
	50 pA	1.778	3.701	1.333	3.041	> 0.9999	0.1312
	75 pA	4.333	4.796	2.889	4.622	0.0664	0.3067
	100 pA	7.667	5.123	4.556	6.307	< **0.0001**	0.5415
	125 pA	10.78	5.044	7.000	6.245	< **0.0001**	0.6655
	150 pA	13.44	5.003	9.556	7.230	< **0.0001**	0.6255
	175 pA	15.67	4.975	11.89	7.672	< **0.0001**	0.5843
	200 pA	18.11	4.781	13.56	8.293	< **0.0001**	0.6730
	225 pA	19.78	5.142	15.78	8.700	< **0.0001**	0.5597
		Control adult		D1R antagonist adult		*p*-value	d
		n = 12				ANOVA2 way	Cohen
		Mean	SD	Mean	SD		
Firing frequency (Hz)	0 pA	0.083	0.289	0.000	0.000	> 0.9999	0.4082
	25 pA	0.833	1.801	2.417	3.753	**0.0046**	0.5379
	50 pA	3.250	4.372	5.667	5.280	< **0.0001**	0.4986
	75 pA	6.750	5.770	7.917	6.653	**0.0481**	0.1873
	100 pA	10.17	6.279	11.92	6.302	**0.0016**	0.2782
	125 pA	13.33	6.679	14.50	5.992	**0.0481**	0.1839
	150 pA	15.75	6.877	16.75	6.092	0.1055	0.1539
	175 pA	18.17	7.554	18.83	6.088	0.3908	0.0972
	200 pA	20.58	7.154	20.83	6.103	> 0.9999	0.0376
	225 pA	22.58	6.868	22.50	6.230	> 0.9999	0.0127

response to a somatic injection of depolarizing currents in the presence of SCH 23390 compared to control conditions (Fig. 5B, two-way repeated measures ANOVA, $F_{(9,\ 72)} = 48.58$, $p < 0.0001$, $n = 9$ and Table 3), as illustrated by the recorded traces (Fig. 5C) and by the frequency/current input–output curve (Fig. 5B). Furthermore, the rheobase of these neurons was significantly higher with SCH 23390 compared to

Table 4. Statistical analysis of the effect of the dopamine D1 receptor agonist and antagonist on the intrinsic properties of layer V pyramidal neurons.

	Control young		D1R agonist young		*P* value	Effect size d
	n = 9				Wilcoxon	Cohen
	Mean	SD	Mean	SD		
Vrest (mV)	−77.09	2.660	−75.75	3.600	0.6523	0.4234
Rheobase (pA)	51.44	28.76	36.00	25.97	**0.0391**	0.5635
Resistance (MΩ)	249.0	65.60	254.0	61.37	0.9102	0.0787
Half width (ms)	0.892	0.178	0.853	0.173	**0.0195**	0.2211
AP threshold (mV)	−51.94	2.297	−54.06	2.877	**0.0039**	0.8144
Peak amplitude (mV)	50.19	6.285	44.54	10.96	**0.0039**	0.6324
	Control adult		D1R agonist adult		*P* value	d
	n = 17				Wilcoxon	Cohen
	Mean	SD	Mean	SD		
Vrest (mV)	−77.92	5.624	−78.34	6.883	0.354	0.0668
Rheobase (pA)	52.12	22.01	49.71	26.87	0.5245	0.0981
Resistance (MΩ)	230.8	56.93	207.6	48.43	0.0505	0.4390
Half width (ms)	0.834	0.111	0.758	0.081	**0.0003**	0.7820
AP threshold (mV)	−52.29	4.024	−54.32	4.896	**0.0242**	0.4530
Peak amplitude (mV)	37.89	10.90	37.23	9.645	0.7119	0.0641
	Control young		D1R antagonist young		*P* value	d
	n = 9				Wilcoxon	Cohen
	Mean	SD	Mean	SD		
Vrest (mV)	−79.93	3.764	−79.73	6.085	0.8203	0.0395
Rheobase (pA)	65.89	28.09	108.3	65.53	**0.0313**	0.8412
Resistance (MΩ)	214.6	53.39	162.2	39.47	**0.0078**	1.1161
Half width (ms)	0.797	0.092	0.755	0.072	**0.0273**	0.5039
AP threshold (mV)	−50.61	2.913	−51.44	3.395	0.2461	0.2624
Peak amplitude (mV)	44.16	8.943	40.63	9.343	**0.027**	0.3860
	Control adult		D1R antagonist adult		*P* value	d
	n = 12				Wilcoxon	Cohen
	Mean	SD	Mean	SD		
Vrest (mV)	−78.39	5.105	−75.23	6.967	**0.0425**	0.5174
Rheobase (pA)	63.08	50.82	45.33	35.40	**0.0425**	0.4053
Resistance (MΩ)	186.7	64.00	187.1	68.04	0.1099	0.0061
Half width (ms)	0.736	0.107	0.696	0.116	0.1294	0.3660
AP threshold (mV)	−53.83	3.284	−55.83	5.623	**0.0337**	0.4559
Peak amplitude (mV)	46.59	9.000	42.22	10.17	0.0640	0.4551

control conditions (WSR, $p < 0.05$, $n = 9$ and Table 4), and the input resistance, the action potential half-width and peak amplitude were significantly lower with SCH 23390 compared to control conditions (Fig. 5D, WSR, $p < 0.05$, $n = 9$). No significant differences were observed concerning the resting membrane potential and the action potential threshold between SCH 23390 and control conditions (Fig. 5D, WSR, $p > 0.05$, $n = 9$).

The same experiments were then performed in adult mice (Fig. 6). Surprisingly, even if the effect size is considered as small (Table 3), the excitability of layer V D1+ PNs was significantly increased by the bath application of the D1 receptor antagonist as it was with the application of the D1 receptor agonist. Indeed, the recorded D1+ PNs fired more action potentials following low-intensity stimulation ranging from 25 pA to 125 pA with 1 μM SCH 23390 than in control conditions (Fig. 6B, C, two-way repeated measures ANOVA, $F_{(9, 99)} = 124.4$, $p < 0.0001$, $n = 12$). Moreover, the resting potential of these neurons was more depolarized in the presence of D1 receptor antagonist SCH 23390 compared to control conditions (Fig. 6D, WSR, $p < 0.05$, $n = 12$ and Table 4). Furthermore, the rheobase and the action potential threshold of layer V M1 D1+ PNs were lowered while blocking D1 receptors (Fig. 6D, WSR, $p < 0.05$, $n = 12$). No significant effects were observed concerning the input resistance, the action potential half-width, and peak amplitude (Fig. 6D, WSR, $p > 0.05$, $n = 12$).

DISCUSSION

DA signaling is crucial for the control of voluntary movement and for motor learning, however, how D1 receptors modulate intrinsic properties of individual neurons in mouse primary motor cortex is poorly

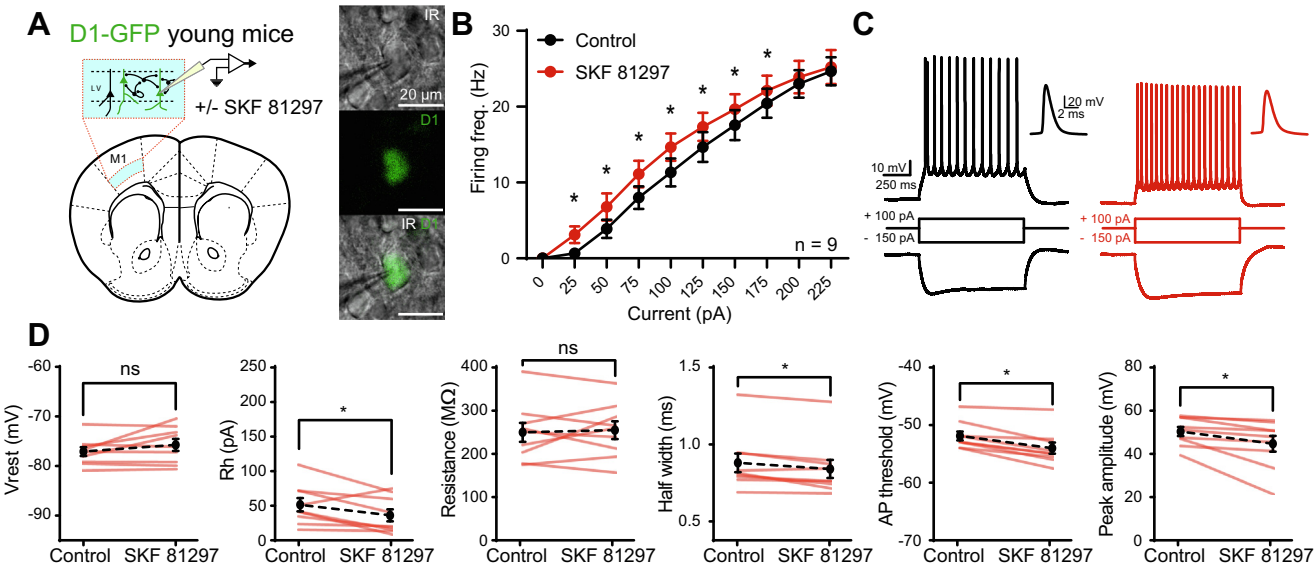

Fig. 3. Effect in M1 of the D1 dopaminergic agonist SKF 81297 on the intrinsic properties of layer V D1+ pyramidal cells in young mice. **(A)** Left, experimental design. Right, images of a recorded pyramidal neuron expressing the D1 receptor under IR-DIC (top, IR), fluorescence (GFP, middle) and merge of the two pictures (down, IR/GFP). **(B)** Input/output curves in control (black) and in presence of the D1 agonist (red). $n = 9$. $^*p < 0.05$ (two-way repeated measures ANOVA). **(C)** Responses to depolarizing and hyperpolarizing current steps in an individual pyramidal neuron recorded before (left) and after bath application of D1 agonist (right, in red). An expanded view of a single spike is presented next to each trace. **(D)** Cell parameters recorded before and after bath application of D1 agonist, from left to right: resting membrane potential, rheobase, input resistance, half-width of action potentials, action potential threshold, and peak amplitude of action potential. $n = 9$. $^*p < 0.05$, ns = non-significant (WSR).

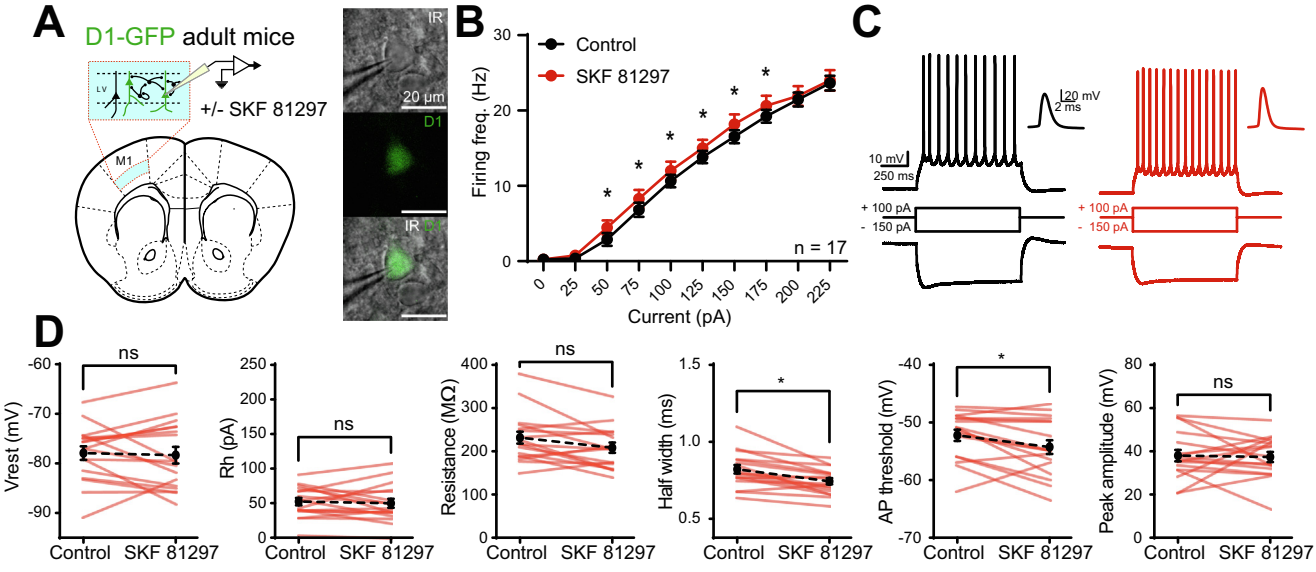

Fig. 4. Effect in M1 of the D1 dopaminergic agonist SKF 81297 on the intrinsic properties of layer V D1+ pyramidal cells in adult mice. **(A)** Left, experimental design. Right, images of a recorded pyramidal neuron expressing the D1 receptor under IR-DIC (top), fluorescence (middle, GFP) and merge of the two pictures (down). **(B)** Input/output curve in control (black) and in presence of the D1 agonist (red). $n = 17$. $^*p < 0.05$ (two-way repeated measures ANOVA). **(C)** Responses to depolarizing and hyperpolarizing current steps in an individual pyramidal neuron recorded before (left) and after bath application of D1 agonist (right). An expanded view of a single spike is presented next to each trace. **(D)** Cell parameters recorded in adult animals before and after bath application of D1 agonist, from left to right: resting membrane potential, rheobase, input resistance, half-width of action potentials, action potential threshold, and peak amplitude of action potential. $n = 17$. $^*p < 0.05$, ns = non-significant (WSR).

understood and contradictory. In this study, we demonstrated *ex vivo* that neurons expressing the D1 receptor are widely distributed in all layers of M1 similarly in young and adult mice. Moreover, we showed that blocking or activating the D1 receptor modulates in a specific way the intrinsic properties of layer V D1+ PNs depending on the age of the animals.

We first showed that D1+ cells are widely distributed in all layers of M1. This distribution correlates well with the localization of the DAergic fibers in the superficial and deep layers of M1 (Berger et al., 1985; Descarries

et al., 1987; Raghanti et al., 2008; Vitrac et al., 2014). As it has been shown in the medial PFC that the expression of the D1 receptor changes during postnatal development (Leslie et al., 1991), we looked at the expression of the D1 receptor in M1 at two stages. The mapping of these D1+ cells reveals a similar distribution regardless of the age of the mice, with however a slight tendency to decrease in superficial layers and to increase in deep layers when mice get older. Projection neurons progressively acquire subtype and area identities by transcriptional mechanisms (for review see Greig et al., 2013). To better characterize the identity of the neurons that express the D1 receptor, we used the classical biological markers of distinct pyramidal neurons, Ctip2 for PT neurons and Satb2 for IT neurons (Arlotta et al., 2005; Alcamo et al., 2008; Britanova et al., 2008; Digilio et al., 2015; for review see Molnár and Cheung, 2006). Satb2 represses the expression or prevents the activity of Ctip2 (Alcamo et al., 2008; Britanova et al., 2008). Thus, overexpression of Satb2 during adolescence in layer II/III could be of importance to repress the expression of other transcriptional factors leading to the specification of neurons other than subcortical- and callosal-projection neurons. Nearly 15% of the cells were expressing only the D1 receptor, suggesting that some inhibitory interneurons and some CT pyramidal neurons in layer VI also express the D1 receptor as described in the PFC (Anastasiades et al., 2019). As very few D1+ neurons express only Ctip2, it indicates that the majority of PT neurons do not have the D1 receptor as already reported (Gaspar et al., 1995; for review see Shepherd, 2013). In any case, most of the D1+ cells also express Satb2 suggesting that a majority of these cells are IT neurons, which is similar with previous findings at the level of the PFC (Anastasiades et al., 2019). Because the D1/Satb2 cells are located in different layers, they could be further identified as IT Cortico-cortical neurons in layer II/III and IT Cortico-striatal neurons in deeper layers (Huang et al., 2013; Shepherd, 2013). As it has already been reported in neocortical regions in mice (McKenna et al., 2011), staining with Ctip2 antibodies revealed neurons that expressed high levels of Ctip2 protein while Ctip2 expression level was much lower in others. Satb2 is known to negatively regulate the level and activity of Ctip2 in neurons (Alcamo et al., 2008; Britanova et al., 2008). Interestingly, some cells co-express Satb2 and Ctip2 in deep layers highlighting the existence of a subpopulation of neurons that have been already described in the somatosensory cortex (Harb et al., 2016), motor area (Sohur et al., 2014; Tantirigama et al., 2014) and hippocampus (Lickiss et al., 2012; Nielsen et al., 2014; Digilio et al., 2015) that also express the D1 receptor.

Using a combination of pharmacology and *ex vivo* electrophysiology, we studied how DA modulates the intrinsic properties of D1+ PNs in layer V of M1 in young and adult mice. Intracellular cascades induced by DAergic receptor activation vary with the cell types and the brain region (Stoof and Kebabian, 1981; Sidhu et al., 1991; Rioult-Pedotti et al., 2015; for review see Mishra et al., 2018) and more importantly, the DA receptor can be coupled with several G proteins (for review see Sidhu, 1998). To avoid a network effect and to specifically study the impact of the D1 receptor on the electrical intrinsic properties of the neurons, we isolated the neurons recorded from the network by the presence of fast synaptic transmission blockers. In this study, we demonstrated

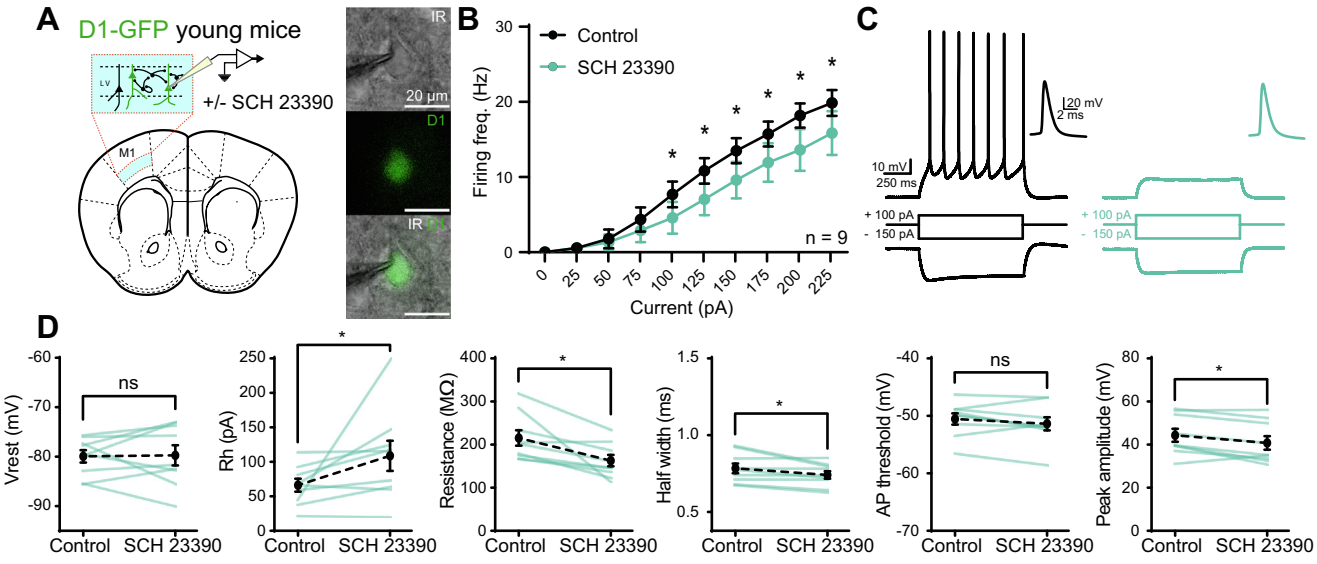

Fig. 5. Effect in M1 of the D1 dopaminergic antagonist SCH 23390 on the intrinsic properties of layer V D1+ pyramidal cells in young mice. **(A)** Left, experimental design. Right, images of a recorded pyramidal neuron expressing the D1 receptor under IR-DIC (top), fluorescence (middle) and merge of the two pictures (down). **(B)** Input/output curves in control (black) and in presence of the D1 antagonist (blue). $n = 9$. $^*p < 0.05$ (two-way repeated measures ANOVA). **(C)** Responses to depolarizing and hyperpolarizing current steps in an individual pyramidal neuron recorded before (left) and after bath application of D1 antagonist (right in blue). An expanded view of a single spike is presented next to each trace. **(D)** Cell parameters recorded in young animals before and after bath application of D1 antagonist, from left to right: resting membrane potential, rheobase, input resistance, half-width of action potentials, action potential threshold and peak amplitude of action potentials. $n = 9$. $^*p < 0.05$, ns = non-significant (WSR).

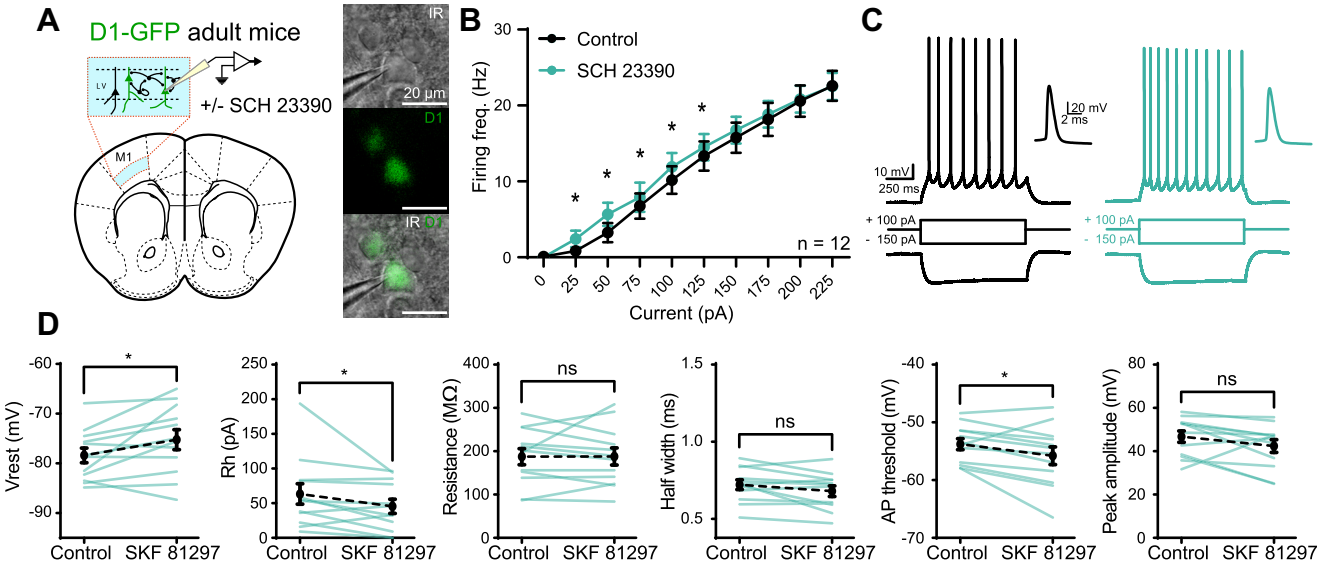

Fig. 6. Effect in M1 of the D1 dopaminergic antagonist SCH 23390 on the intrinsic properties of layer V D1+ pyramidal cells in adult mice. **A**. Left, experimental design. Right, images of a recorded pyramidal neuron expressing the D1 receptor under IR-DIC (top), fluorescence (middle) and merge of the two pictures (down). **(B)** Input/output curves in control (black) and in presence of the D1 antagonist (green). $n = 12$. *$p < 0.05$ (two-way repeated measures ANOVA). **(C)** Responses to depolarizing and hyperpolarizing current steps in an individual pyramidal neuron recorded before (left) and after bath application of D1 antagonist (right in blue). An expanded view of a single spike is presented next to each trace. **(D)** Cell parameters recorded in adult animals before and after bath application of D1 antagonist, from left to right: resting membrane potential, rheobase, input resistance, half width of action potential, action potential threshold and peak amplitude of action potential. $n = 12$. *$p < 0.05$, ns = non-significant (WSR).

that activating the D1 receptor increased the excitability of M1 layer V D1+ PNs, presumably IT, both in young and adult mice. These results concur with previous findings in PFC; where it has been demonstrated that the activation of D1 receptor can directly modulate the firing properties of subpopulation of PNs in layer V (Seong and Carter, 2012), mainly IT (Anastasiades et al., 2019). However, even if we observed a significant global change in intrinsic properties, we observed an important inter-individual variability of the responses induced by the bath application of the agonist. Even if the immunohistochemistry experiments (Figs. 1, 2) indicate that most of the D1+ cells in layer V of M1 are IT neurons, this variability suggests that subtypes of D1+ PNs have been recorded (Sohur et al., 2014; Tantirigama et al., 2014). More specifically, a small portion of recorded cells may be PT neurons, as it has been shown that PT neurons in the layer V of the mouse PFC can also express D1 receptors (Leyrer-Jackson and Thomas, 2019). At first glance, these results do not seem to agree with an *in vivo* study showing a decrease in excitability of layer V PNs following DA local application in rat motor cortex (Awenowicz and Porter, 2002), but their study was targeting specifically PT neurons whereas our recordings were done in a majority of IT neurons.

Interestingly, we demonstrated an age-dependent action of D1 receptor antagonist on intrinsic electrical properties of layer V D1+ PNs. While D1 receptor blockade decreased the excitability of M1 layer V D1+ PNs in young animals, it increased their excitability in adults. In young mice, as the D1 receptor activation induced an increase in M1 layer V D1+ PNs excitability, it was consistent to observe a decrease in the excitability of M1 layer V D1+ PNs by the blockade of the D1 receptor. This supports the idea that the D1 receptors recruit an excitatory G protein. Surprisingly, in adults, the D1 receptor blockade increased the firing frequency and lowered the action potential threshold of M1 layer V D1+ PNs as it was for the activation of the D1 receptor. Even if it is surprising, the effect observed in adults is in line with the work of Swanson and colleagues who recently showed *ex vivo* that D1 receptor antagonism caused increased excitability of layer V PNs with the engagement of intrinsic mechanisms (Swanson et al., 2021). This electrophysiological signature in the presence of the antagonist is reminiscent of the altered electrophysiological properties (*i.e.*, higher firing frequency and depolarized resting membrane potential) described *in vivo* in cortical neurons of Parkinsonian rats in which the DAergic transmission was interrupted (Degos et al., 2013). While in young mice, concomitant use of the D1 agonist and D1 antagonist can cancel each other's action, the lack of effect on excitability in adult mice is surprising, since both, when used separately, increase the excitability of D1+ PN neurons. Moreover, why the D1 receptor antagonists produce the opposite effect on M1 D1+ PNs in young and adult animals is not easy to explain but some hypothesis can be raised. Besides, drug effects on receptor activity are often integrated with some preexisting level of receptor activity which depends on endogenous ligand and constitutive receptor activity. It has been already reported that the D1 receptor in other brain regions can have a constitutive activity (Rankin et al., 2006; Zhang et al., 2014) meaning a receptor activity in the absence of ligands at the binding site. The opposite effect observed in young and adult mice may suggest that the D1 receptor could

be constitutively active in adults but not in young animals. This hypothesis is reinforced by the fact that the effects observed in adults by the bath application of D1 receptor agonist were not as strong as the ones observed in young animals as attested by the measure of the size effect (Table 3). Indeed, if the constitutive activity of the receptor in adult is high, further increasing the activity of the receptor by the agonist may have a small effect relative to the baseline and may be harder to detect. Additionally, the effect of the antagonist will work better if there is a high level of DA. The data obtained could thus suggest a different DAergic tone in young and adult mice that could arise from different emotional or motor states, but there is no proof at this date of a different DA tone in the M1 of mice depending of the age. Thus, the DAergic modulation may be governed by different mechanisms at different ages which can involve intricate interactions between level of endogenous ligands, constitutive activity and distinct intrinsic pathways.

In summary, this study unravels the impact of D1 receptors on M1 layer V PNs *ex vivo*, and maps for the first time the D1 receptor-expressing neurons in M1 according to their molecular profile. The D1 receptors modulation of M1 layer V PNs is of importance for the physiological completion of M1 processes, such as motor learning and execution of fine motor tasks in a healthy M1 and impaired DA signaling will lead to pathologies.

DECLARATION OF COMPETING INTEREST

The authors declare that they have no known competing financial interests or personal relationships that could have appeared to influence the work reported in this paper.

ACKNOWLEDGEMENTS

This work was supported by the University of Bordeaux, the CNRS (Centre National de la Recherche Scientifique), the French government through the University of Bordeaux's IdEx "Investments for the Future" program/GPR BRAIN_2030 (to J.B. and M. L. B. J.), and the Bordeaux Neurocampus Department (Seed project Damoco). V.P. benefitted from the help of the Bordeaux Neurocampus Graduate Program, managed by the French National Research Agency reference ANR-17-EURE-0028. Confocal images were taken at the Bordeaux imaging center.

REFERENCES

Albin RL, Young AB, Penney JB (1989) The functional anatomy of basal ganglia disorders. Trends Neurosci 12:366–375. Available from: https://academic.oup.com/jhered/article/109/6/700/5035183.

Alcamo EA, Chirivella L, Dautzenberg M, Dobreva G, Fariñas I, Grosschedl R, McConnell SK (2008) Satb2 Regulates Callosal Projection Neuron Identity in the Developing Cerebral Cortex. Neuron 57:364–377. Available from: https://linkinghub.elsevier.com/retrieve/pii/S0896627307010173.

Alm PA (2021) The Dopamine System and Automatization of Movement Sequences: A Review With Relevance for Speech and Stuttering. Front Hum Neurosci 15:1–17. https://doi.org/10.3389/fnhum.2021.661880/full.

Anastasiades PG, Boada C, Carter AG (2019) Cell-Type-Specific D1 Dopamine Receptor Modulation of Projection Neurons and Interneurons in the Prefrontal Cortex. Cereb Cortex 29:3224–3242. Available from: https://academic.oup.com/cercor/article/29/7/3224/5253209.

Arlotta P, Molyneaux BJ, Chen J, Inoue J, Kominami R, Macklis JD (2005) Neuronal Subtype-Specific Genes that Control Corticospinal Motor Neuron Development In Vivo. Neuron 45:207–221. Available from: https://linkinghub.elsevier.com/retrieve/pii/S0896627304008530.

Aronoff R, Matyas F, Mateo C, Ciron C, Schneider B, Petersen CCH (2010) Long-range connectivity of mouse primary somatosensory barrel cortex. Eur J Neurosci 31:2221–2233. https://doi.org/10.1111/j.1460-9568.2010.07264.x.

Awenowicz PW, Porter LL (2002) Local application of dopamine inhibits pyramidal tract neuron activity in the rodent motor cortex. J Neurophysiol 88:3439–3451.

Berger B, Verney C, Alvarez C, Vigny A, Helle KB (1985) New dopaminergic terminal fields in the motor, visual (area 18b) and retrosplenial cortex in the young and adult rat. Immunocytochemical and catecholamine histochemical analyses. Neuroscience 15:983–998. Available from: https://linkinghub.elsevier.com/retrieve/pii/0306452285902489.

Bernheimer H, Birkmayer W, Hornykiewicz O, Jellinger K, Seitelberger F (1973) Brain dopamine and the syndromes of Parkinson and Huntington Clinical, morphological and neurochemical correlations. J Neurol Sci 20:415–455.

Bernheimer H, Hornykiewicz O (1965) Decreased homovanillic acid concentration in the brain in parkinsonian subjects as an expression of a disorder of central dopamine metabolism. Klin Wochenschr 43:711–715. https://doi.org/10.1007/BF01707066.

Botvinick M, Braver T (2015) Motivation and Cognitive Control: From Behavior to Neural Mechanism. Annu Rev Psychol 66:83–113. https://doi.org/10.1146/annurev-psych-010814-015044.

Brisch R, Saniotis A, Wolf R, Bielau H, Bernstein H-G, Steiner J, Bogerts B, Braun AK, Jankowski Z, Kumaritlake J, Henneberg M, Gos T (2014) The Role of Dopamine in Schizophrenia from a Neurobiological and Evolutionary Perspective: Old Fashioned, but Still in Vogue. Front Psychiatry 5:1–11. https://doi.org/10.3389/fpsyt.2014.00047/abstract.

Britanova O, de Juan Romero C, Cheung A, Kwan KY, Schwark M, Gyorgy A, Vogel T, Akopov S, Mitkovski M, Agoston D, Šestan N, Molnár Z, Tarabykin V (2008) Satb2 Is a Postmitotic Determinant for Upper-Layer Neuron Specification in the Neocortex. Neuron 57:378–392. Available from: https://linkinghub.elsevier.com/retrieve/pii/S0896627308000330.

Brown AS, Gershon S (1993) Dopamine and depression. J Neural Transm 91:75–109. https://doi.org/10.1002/hup.470100510.

Chudasama Y, Robbins TW (2004) Dopaminergic Modulation of Visual Attention and Working Memory in the Rodent Prefrontal Cortex. Neuropsychopharmacology 29:1628–1636. Available from: http://www.nature.com/articles/1300490.

Cohen J (1988). Statistical Power Analysis for the Behavioral Sciences. New York: NY: Routledge Academic. https://books.google.fr/books?hl=en&lr=&id=rEe0BQAAQBAJ&oi=fnd&pg=PP1&ots=sw0XPxQQm5&sig=rSI761-lqW_9pkPCqUkrukCmEfs&redir_esc=y#v=onepage&q&f=false.

Cousineau J, Lescouzères L, Taupignon A, Delgado-Zabalza L, Valjent E, Baufreton J, Le Bon-Jégo M (2020) Dopamine D2-Like Receptors Modulate Intrinsic Properties and Synaptic Transmission of Parvalbumin Interneurons in the Mouse Primary Motor Cortex. Eneuro 7. https://doi.org/10.1523/ENEURO.0081-20.2020 ENEURO.0081-20.2020.

Cousineau J, Plateau V, Baufreton J, Le Bon-Jégo M (2022) Dopaminergic modulation of primary motor cortex: From cellular and synaptic mechanisms underlying motor learning to cognitive symptoms in Parkinson's disease. Neurobiol Dis 167:105674.

Available from: https://linkinghub.elsevier.com/retrieve/pii/S0969996122000651.
D'Ardenne K, Eshel N, Luka J, Lenartowicz A, Nystrom LE, Cohen JD (2012) Role of prefrontal cortex and the midbrain dopamine system in working memory updating. Proc Natl Acad Sci 109:19900–19909. https://doi.org/10.1073/pnas.1116727109.
Davis KL, Kahn RS, Ko G, Davidson M (1991) Dopamine in schizophrenia: a review and reconceptualization. Am J Psychiatry 148:1474–1486. https://doi.org/10.1176/ajp.148.11.1474.
Dawson T, Gehlert D, McCabe R, Barnett A, Wamsley J (1986) D-1 dopamine receptors in the rat brain: a quantitative autoradiographic analysis. J Neurosci 6:2352–2365. https://doi.org/10.1523/JNEUROSCI.06-08-02352.1986.
Degos B, Deniau J-M, Chavez M, Maurice N (2013) Subthalamic Nucleus High-Frequency Stimulation Restores Altered Electrophysiological Properties of Cortical Neurons in Parkinsonian Rat. PLoS One 8:e83608. https://doi.org/10.1371/journal.pone.0083608.
Descarries L, Lemay B, Doucet G, Berger B (1987) Regional and laminar density of the dopamine innervation in adult rat cerebral cortex. Neuroscience 21:807–824. Available from: https://linkinghub.elsevier.com/retrieve/pii/0306452287900388.
Diamond A (1996) Evidence for the importance of dopamine for prefrontal cortex functions early in life. Philos Trans R Soc London Ser B Biol Sci 351:1483–1494. https://doi.org/10.1098/rstb.1996.0134.
Digilio L, Yap CC, Winckler B (2015) Ctip2-, Satb2-, Prox1-, and GAD65-Expressing Neurons in Rat Cultures: Preponderance of Single- and Double-Positive Cells, and Cell Type-Specific Expression of Neuron-Specific Gene Family Members, Nsg-1 (NEEP21) and Nsg-2 (P19). PLoS One 10:e0140010. Available from: http://www.ncbi.nlm.nih.gov/pubmed/26465886.
Floresco SB (2013) Prefrontal dopamine and behavioral flexibility: shifting from an ''inverted-U" toward a family of functions. Front Neurosci 7:1–12. https://doi.org/10.3389/fnins.2013.00062/abstract.
Gaspar P, Bloch B, Moine C (1995) D1 and D2 Receptor Gene Expression in the Rat Frontal Cortex: Cellular Localization in Different Classes of Efferent Neurons. Eur J Neurosci 7:1050–1063. https://doi.org/10.1111/j.1460-9568.1995.tb01092.x.
Gaspar P, Duyckaerts C, Alvarez C, Javoy-Agid F, Berger B (1991) Alterations of dopaminergic and noradrenergic innervations in motor cortex in parkinson's disease. Ann Neurol 30:365–374.
Grace AA (2016) Dysregulation of the dopamine system in the pathophysiology of schizophrenia and depression. Nat Rev Neurosci 17:524–532. https://doi.org/10.1038/nrn.2016.57.
Greig LC, Woodworth MB, Galazo MJ, Padmanabhan H, Macklis JD (2013) Molecular logic of neocortical projection neuron specification, development and diversity. Nat Rev Neurosci 14:755–769. https://doi.org/10.1038/nrn3586.
Guo L, Xiong H, Kim J-I, Wu Y-W, Lalchandani RR, Cui Y, Shu Y, Xu T, Ding JB (2015) Dynamic rewiring of neural circuits in the motor cortex in mouse models of Parkinson's disease. Nat Neurosci 18:1299–1309. https://doi.org/10.1093/brain/aws124.
Harb K, Magrinelli E, Nicolas CS, Lukianets N, Frangeul L, Pietri M, Sun T, Sandoz G, Grammont F, Jabaudon D, Studer M, Alfano C (2016) Area-specific development of distinct projection neuron subclasses is regulated by postnatal epigenetic modifications. Elife 5:1–25. Available from: https://elifesciences.org/articles/09531.
Harris KD, Shepherd GMG (2015) The neocortical circuit: themes and variations. Nat Neurosci 18:170–181. Available from: http://www.nature.com/articles/nn.3917.
Hattox AM, Nelson SB (2007) Layer V Neurons in Mouse Cortex Projecting to Different Targets Have Distinct Physiological Properties. J Neurophysiol 98:3330–3340. https://doi.org/10.1152/jn.00397.2007.
Hosp JA, Molina-Luna K, Hertler B, Atiemo CO, Luft AR (2009) Dopaminergic Modulation of Motor Maps in Rat Motor Cortex: An In Vivo Study. Neuroscience 159:692–700. https://doi.org/10.1016/j.neuroscience.2008.12.056.
Hosp JA, Nolan HE, Luft AR (2015) Topography and collateralization of dopaminergic projections to primary motor cortex in rats. Exp Brain Res 233:1365–1375. Available from: http://www.ncbi.nlm.nih.gov/pubmed/25633321.
Hosp JA, Pekanovic A, Rioult-Pedotti MS, Luft AR (2011) Dopaminergic Projections from Midbrain to Primary Motor Cortex Mediate Motor Skill Learning. J Neurosci 31:2481–2487. https://doi.org/10.1523/JNEUROSCI.5411-10.2011.
Huang Y, Song N-N, Lan W, Hu L, Su C-J, Ding Y-Q, Zhang L (2013) Expression of Transcription Factor Satb2 in Adult Mouse Brain. Anat Rec 296:452–461. Available from: https://onlinelibrary.wiley.com/doi/10.1002/ar.22656.
Leslie CA, Robertson MW, Cutler AJ, Bennett JP (1991) Postnatal development of D 1 dopamine receptors in the medial prefrontal cortex, striatum and nucleus accumbens of normal and neonatal 6-hydroxydopamine treated rats: a quantitative autoradiographic analysis. Dev Brain Res 62:109–114. Available from: https://linkinghub.elsevier.com/retrieve/pii/016538069190195O.
Lévesque M, Gagnon S, Parent A, Deschênes M (1996) Axonal Arborizations of Corticostriatal and Corticothalamic Fibers Arising from the Second Somatosensory Area in the Rat. Cereb Cortex 6:759–770. https://doi.org/10.1093/cercor/6.6.759.
Leyrer-Jackson JM, Thomas MP (2019) Dopaminergic D1 receptor effects on commissural inputs targeting layer V pyramidal subtypes of the mouse medial prefrontal cortex. Physiol Rep 7:1–12. https://doi.org/10.14814/phy2.14256.
Lickiss T, Cheung AFP, Hutchinson CE, Taylor JSH, Molnár Z (2012) Examining the relationship between early axon growth and transcription factor expression in the developing cerebral cortex. J Anat 220:201–211. https://doi.org/10.1111/j.1469-7580.2011.01466.x.
Lidow MS, Goldman-Rakic PS, Rakic P, Innis RB (1989) Dopamine D2 receptors in the cerebral cortex: distribution and pharmacological characterization with [3H]raclopride. Proc Natl Acad Sci 86:6412–6416. https://doi.org/10.1073/pnas.86.16.6412.
McKenna WL, Betancourt J, Larkin KA, Abrams B, Guo C, Rubenstein JLR, Chen B (2011) Tbr1 and Fezf2 Regulate Alternate Corticofugal Neuronal Identities during Neocortical Development. J Neurosci 31:549–564. https://doi.org/10.1523/JNEUROSCI.4131-10.2011.
Michely J, Viswanathan S, Hauser TU, Delker L, Dolan RJ, Grefkes C (2020) The role of dopamine in dynamic effort-reward integration. Neuropsychopharmacology 45:1448–1453. https://doi.org/10.1038/s41386-020-0669-0.
Mishra A, Singh S, Shukla S (2018) Physiological and Functional Basis of Dopamine Receptors and Their Role in Neurogenesis: Possible Implication for Parkinson's disease. J Exp Neurosci 12. https://doi.org/10.1177/1179069518779829 117906951877982.
Molnár Z, Cheung AFP (2006) Towards the classification of subpopulations of layer V pyramidal projection neurons. Neurosci Res 55:105–115. Available from: https://linkinghub.elsevier.com/retrieve/pii/S0168010206000447.
Nambu A, Tachibana Y, Chiken S (2015) Cause of parkinsonian symptoms: Firing rate, firing pattern or dynamic activity changes? Basal Ganglia 5:1–6. https://doi.org/10.1016/j.baga.2014.11.001.
Nielsen JV, Thomassen M, Møllgård K, Noraberg J, Jensen NA (2014) Zbtb20 Defines a Hippocampal Neuronal Identity Through Direct Repression of Genes That Control Projection Neuron Development in the Isocortex. Cereb Cortex 24:1216–1229. https://doi.org/10.1093/cercor/bhs400.
Nieoullon A (2002) Dopamine and the regulation of cognition and attention. Prog Neurobiol 67:53–83. Available from: https://linkinghub.elsevier.com/retrieve/pii/S0301008202000114.
Ott T, Nieder A (2019) Dopamine and Cognitive Control in Prefrontal Cortex. Trends Cogn Sci 23:213–234. https://doi.org/10.1016/j.tics.2018.12.006.

Parr-Brownlie LC (2005) Bradykinesia Induced by Dopamine D2 Receptor Blockade Is Associated with Reduced Motor Cortex Activity in the Rat. J Neurosci 25:5700–5709. https://doi.org/10.1523/JNEUROSCI.0523-05.2005.

Raghanti MA, Stimpson CD, Marcinkiewicz JL, Erwin JM, Hof PR, Sherwood CC (2008) Cortical dopaminergic innervation among humans, chimpanzees, and macaque monkeys: a comparative study. Neuroscience 155:203–220. Available from: http://www.ncbi.nlm.nih.gov/pubmed/18562124.

Rankin ML, Marinec PS, Cabrera DM, Wang Z, Jose PA, Sibley DR (2006) The D 1 Dopamine Receptor Is Constitutively Phosphorylated by G Protein-Coupled Receptor Kinase 4. Mol Pharmacol 69:759–769. https://doi.org/10.1124/mol.105.019901.

Rioult-Pedotti M-S, Pekanovic A, Atiemo CO, Marshall J, Luft AR (2015) Dopamine Promotes Motor Cortex Plasticity and Motor Skill Learning via PLC Activation. PLoS One 10:e0124986. https://doi.org/10.1371/journal.pone.0124986.

Robbins TW, Everitt BJ (1992) Functions of dopamine in the dorsal and ventral striatum. Semin Neurosci 4:119–127.

Salamone JD (1992) Complex motor and sensorimotor functions of striatal and accumbens dopamine: involvement in instrumental behavior processes. Psychopharmacology (Berl) 107:160–174. https://doi.org/10.1007/BF02245133.

Seong HJ, Carter AG (2012) D1 Receptor Modulation of Action Potential Firing in a Subpopulation of Layer 5 Pyramidal Neurons in the Prefrontal Cortex. J Neurosci 32:10516–10521. https://doi.org/10.1523/JNEUROSCI.1367-12.2012.

Shepherd GMG (2013) Corticostriatal connectivity and its role in disease. Nat Rev Neurosci 14:278–291. https://doi.org/10.1038/nrn3469.

Sidhu A (1998) Coupling of D1 and D5 dopamine receptors to multiple G proteins. Mol Neurobiol 16:125–134.

Sidhu A, Sullivan M, Kohout T, Balen P, Fishman PH (1991) D 1 Dopamine Receptors Can Interact with Both Stimulatory and Inhibitory Guanine Nucleotide Binding Proteins. J Neurochem 57:1445–1451. https://doi.org/10.1111/j.1471-4159.1991.tb08312.x.

Sohur US, Padmanabhan HK, Kotchetkov IS, Menezes JRL, Macklis JD (2014) Anatomic and Molecular Development of Corticostriatal Projection Neurons in Mice. Cereb Cortex 24:293–303. https://doi.org/10.1093/cercor/bhs342.

Stoof JC, Kebabian JW (1981) Opposing roles for D-1 and D-2 dopamine receptors in efflux of cyclic AMP from rat neostriatum. Nature 294:366–368. Available from: http://www.nature.com/articles/294366a0.

Swanson OK, Semaan R, Maffei A (2021) Reduced Dopamine Signaling Impacts Pyramidal Neuron Excitability in Mouse Motor Cortex. Eneuro 8. https://doi.org/10.1523/ENEURO.0548-19.2021 ENEURO.0548-19.2021.

Tantirigama MLS, Oswald MJ, Duynstee C, Hughes SM, Empson RM (2014) Expression of the Developmental Transcription Factor Fezf2 Identifies a Distinct Subpopulation of Layer 5 Intratelencephalic-Projection Neurons in Mature Mouse Motor Cortex. J Neurosci 34:4303–4308. https://doi.org/10.1523/JNEUROSCI.3111-13.2014.

Ungerstedt U, Butcher LL, Butcher SG, Anden N-E, Fuxe K (1969) Direct chemical stimulation of dopaminergic mechanisms in the neostriatum of the rat. Brain Res 14:461–471. Available from: https://linkinghub.elsevier.com/retrieve/pii/000689936990122X.

Valjent E, Biever A, Gangarossa G, Puighermanal E (2019) Dopamine signaling in the striatum. In: Advances in Protein Chemistry and Structural Biology. Elsevier Inc.. p. 375–396. https://doi.org/10.1016/bs.apcsb.2019.01.004.

Veinante P, Lavallée P, Deschênes M (2000) Corticothalamic projections from layer 5 of the vibrissal barrel cortex in the rat. J Comp Neurol 424:197–204. https://doi.org/10.1002/1096-9861(20000821)424:2%3C197::AID-CNE1%3E3.0.CO;2-6.

Vitrac C, Péron S, Frappé I, Fernagut P-O, Jaber M, Gaillard A, Benoit-Marand M (2014) Dopamine control of pyramidal neuron activity in the primary motor cortex via D2 receptors. Front Neural Circuits 8:1–8. https://doi.org/10.3389/fncir.2014.00013/abstract.

Weiner DM, Levey AI, Sunahara RK, Niznik HB, O'Dowd BF, Seeman P, Brann MR (1991) D1 and D2 dopamine receptor mRNA in rat brain. Proc Natl Acad Sci 88:1859–1863. https://doi.org/10.1073/pnas.88.5.1859.

Yokel RA, Wise RA (1975) Increased Lever Pressing for Amphetamine After Pimozide in Rats: Implications for a Dopamine Theory of Reward. Science (80-) 187:547–549. https://doi.org/10.1126/science.1114313.

Zhang B, Albaker A, Plouffe B, Lefebvre C, Tiberi M (2014) Constitutive Activities and Inverse Agonism in Dopamine Receptors. In: Advances in Pharmacology. Elsevier Inc.. p. 175–214. https://doi.org/10.1016/B978-0-12-417197-8.00007-9.

APPENDIX A. SUPPLEMENTARY MATERIAL

Supplementary material to this article can be found online at https://doi.org/10.1016/j.neuroscience.2023.11.006.

(Received 5 June 2023, Accepted 7 November 2023)
(Available online 11 November 2023)